International Journal of the Physical Sciences Vol. 5(10), pp. 1508-1523, 4 September, 2010
Available online at http://www.academicjournals.org/IJPS
ISSN 1992 - 1950 ©2010 Academic Journals

Full Length Research Paper

Multiphoton angular distribution: Occurrence of an isotropic term and effect of light polarization

Mamadou Faye*, Sada Tamimou Wane and Samba Ndiaye

Groupe de Recherche en Physique Théorique, Atomique et Nucléaire, Département de Physique, Faculté des Sciences et techniques, Université Cheikh Anta Diop, de Dakar, Senegal.

Accepted 20 May, 2010

Within the framework of perturbation theory and of dipole approximation, the angular distribution for third order processes can be expressed for any state of quantum numbers (n, l) of the hydrogen atom as $a+b\cos^2\theta+c\cos^4\theta+d\cos^6\theta$; whatever the polarisation state (linear or circular). The explicit expressions of the corresponding angular coefficients are given for ns and np initial states. It is shown for the particular case of linear polarization that, the isotropic term a occurs only for initial states with orbital quantum number l greater than zero, and contains exactly twenty one contributing terms for np states; in the case of circularly polarized light, the distribution follows a $\sin^6\theta$ behaviour for ns states, while for np states, it is expressed as a combination of $\sin^4\theta$ and $\sin^6\theta$. Using the implicit summation technique, nine radial transitions matrix elements are determined and a quantitative analysis of these coefficients is made for 1s, 2s, 3s, 2p and 3p initial states at various wavelengths, including the three photons ionization threshold; for linear polarization, the shapes are strongly dependent on both quantum numbers (n, l); while for circular polarization the shapes remain the same. Furthermore, the corresponding total cross sections obtained indirectly from these coefficients, are globally in agreement with that obtained directly from other methods.

Key words: Multiphoton, ionization, angular distribution, total cross section, polarization.

INTRODUCTION

It is well known that the study of the angular distribution of photoelectrons can provide information about quantities characterizing the bound and continuum states of the atoms. Odd order non resonant multiphoton ionization (or detachment) processes are of particular interest with the advent of powerful lasers. Experimental investigations for non resonant angular distributions of xenon (Fabre et al., 1981), sodium (Leuch and Smith, 1982), caesium (Dodhy et al., 1985), and rubidium (Dodhy et al., 1986), atoms, have been done using an odd number of linearly polarized photons. All of them exhibit a nonzero distribution at right angle (between laser polarization and the direction of ejected photoelectron), whereas theory (Lambropoulos, 1972), (Gontier et al., 1975) predicts zero distribution. It would be very exciting to study other excited states, so as to verify under what conditions, the isotropic terms is expected to occur; especially as, this nonzero isotropic term has also been observed in xenon (Giugni, 2000).

In the particular case of non resonant three photons ionization of hydrogen atom, for which exact calculations are feasible, calculations emphasizing on other states than the ns ones were similar to those of Arnous et al. (1973), for two photons ionization since these works would be absent in the literature. So, to fill this gap, our aim here is: Firstly, we extend these previous calculations (Lambropoulos, 1972; Gontier et al., 1975) to initial state with a principal quantum number n = 1, 2 and 3 and an orbital quantum number *l* = 0, 1; using linearly as well as circularly polarized light, by expressing the angular distribution, independently of the azimuthal angle (Lambropoulos, 1972), in the universal from:

$a+b\cos^2\theta+c\cos^4\theta+d\cos^6\theta$; as stated by Yang

*Corresponding author. E-mail: mamadou.faye@ucad.edu.sn. Tel: (221)338250444. Fax: (221)338246318.

(1948) general theorem, a long time ago.

Secondly, we determine nine radial transitions matrix elements for 1s, 2s, 3s 2p and 3p; at wavelengths comprising between the two and three photons ionization thresholds as well as three photon threshold ionization. However, the evaluation of the relevant transition matrix elements between complete sets of atomic states (discrete as well as continuum states) is crucial. But, the integration over the continuum poses some difficulty. Various methods (Morellec et al., 1982; Gao and Starace, 1988) have been proposed to calculate these above radial transition matrix elements: Sturmian functions, variational, inhomogeneous differential equations, and recently, Radhakrishnam and Thayyullathhil (2004) have proposed an alternative closed form method. But in general, no one has given the contributions of the angular coefficients to the total cross sections.

In this work, we use the implicit summation technique method, previously used by Zernik and Klopfenstein (1965), and generalized later by Gontier and Trahin (1971) to continue the work of Gontier et al. (1975), only limited to 1s, and 2s states. These calculations devoted to the excited states are very useful in astrophysics (Leckrone and Sugar, 1993).

Furthermore, the corresponding general expressions of the total cross sections for any (n, *l*) initial states have already been given by Maquet (1977), for linear and circular light polarization; in contrast to the present numerical method, he evaluated the radial part with the help of the Coulomb Green's function for ns, np and nd initial states.

In this study, we recall briefly the expressions of the partial amplitudes transitions appearing in the angular distribution for linear and circular polarization and the implicit summation technique used to evaluate the radial part.

We then proceed with derivation of: Firstly, the general analytical expressions of the angular distribution by averaging over the magnetic quantum number m the quadratic and the crossed partial amplitudes, for linearly as well for circularly polarized light. These expressions allow us to arrive at the exact explicit expressions of the angular coefficients (a, b, c, d, c', d'), in the particular cases of ns and np initial states; secondly, the series solutions of the implicit summation technique and the corresponding expressions of the transition matrix elements, are given. So, these coefficients are numerically evaluated from a computer Mathcad 13 program, and discussed at various wavelengths including threshold, for 1s, 2s, 3s, 2p, and 3p states. Finally, we conclude the study.

ANGULAR DISTRIBUTION CALCULATIONS

Within the framework of the perturbation theory and of the dipole approximation, the differential cross section for non resonant three photon ionization (or detachment) has the general form in atomic units:

$$\frac{d\sigma}{1^2 d\Omega} = \frac{\alpha}{2\pi} a_0^2 \left(\frac{1}{2I_0}\right)^2 \omega k \left| \sum_{s_1 s_2} \frac{\left\langle f \left| \vec{\in}.\vec{r} \right| s_2 \right\rangle \left\langle s_2 \left| \vec{\in}.\vec{r} \right| s_1 \right\rangle \left\langle s_1 \left| \vec{\in}.\vec{r} \right| i \right\rangle}{(E_i + 2\omega - E_{s2})(E_i + \omega - E_{s1})} \right|^2 \quad (1)$$

Where α is the fine structure constant, $a_0 = 5.2917 \times 10^{-9}$ cm is the radius of the first Bohr orbit, I the field strength of the radiation, $I_0 = 7.019 \times 10^{16} W/cm^2$ is the atomic unit field strength intensity, k is the momentum of the photoelectron ejected in the direction of the unit vector. The summation runs over the whole (discrete and continuum) spectrum of the unperturbed atomic Hamiltonian and the magnitude of k is given by conservation of energy:

$$\frac{k^2}{2} = E_i + 3\omega$$

Here ε is the unit polarization vector of the incident radiation field, and E_i is the energy of the initial atomic bound state and ω is the energy of the incoming photons. The atomic system is presumed to be initially in an arbitrary bound state (n, *l*, m)

$$\left\langle \vec{r} \middle| \vec{i} \right\rangle = \left\langle \vec{r} \middle| nml \right\rangle = R_{n,1} Y_{1,m}\left(\vec{r}\right)$$

The intermediate (virtual) states $|s_i>$ are belonging to the complete set eigen states:

$$\left\langle \vec{r} \middle| \vec{s}_i \right\rangle = \left\langle \vec{r} \middle| \nu_i \lambda_i \mu_i \right\rangle = R_{vi\lambda i}(r) Y_{\lambda i,\mu i}\left(\vec{r}\right)$$

and the wave function of the photoelectron

$$\left\langle \vec{r} \middle| \vec{f} \right\rangle = \left\langle \vec{r} \middle| \vec{k} \right\rangle$$

is given as the partial wave expression:

$$\left\langle \vec{r} \middle| \vec{k} \right\rangle = \left(\frac{8\pi^3}{k}\right)^{\frac{1}{2}} \sum_{LM} i^L e^{-i\delta L} R_{k,L}(r) Y_{L;M}\left(\vec{r}\right) Y^*_{L;M}(\vec{k})$$

Where

$$\delta_L = \arg\Gamma(L + 1 - \frac{i}{k})$$

is the coulomb phase shift and R_{kL} is the radial wave function

Angular part

With a convenient choice of the coordinate system orientation different from that of
(Lambropoulos, 1972), one shows that the dipole interaction operator assumes the form by Arnous et al. (1973):
For linear polarization

$$\vec{\varepsilon}.\vec{r} = \left(\frac{4\pi}{3}\right)^{1/2} r Y_{1,0}(\vec{r})$$

and, for circular polarization

$(4\pi/3)^{1/2}$

The angular distribution calculation is thus reduced to the evaluation of known integrals over a product of three spherical harmonics. Such integrals may be expressed in terms of Wigner 3 – j symbol (Sobel'man, 1972), one easily gets:

$$\left(\frac{4\pi}{3}\right)^{\frac{1}{2}}\left\langle Y_{\lambda,m}\middle|Y_{1,0}\middle|Y_{1,m}\right\rangle=\left(\frac{l_{\rangle}^{2}-m^{2}}{(2l+1)(2\lambda+1)}\right)^{\frac{1}{2}}$$

$l_{>}$ = sup (l, λ)

$$\left(\frac{4\pi}{3}\right)^{\frac{1}{2}}\left\langle Y_{\lambda,m}\middle|Y_{1,1}\middle|Y_{1,m}\right\rangle=\left(\frac{(l+m+1)(\lambda+1+m)}{2(2l+1)(2\lambda+1)}\right)^{\frac{1}{2}}\delta_{\lambda,l+1}-\left(\frac{(l-m+1)(\lambda+1-m)}{2(2l+1)(2\lambda+1)}\right)^{\frac{1}{2}}\delta_{\lambda,1-1}$$

As a consequence of the selection rules λ = l ± 1, the sum of Equation (1) can be split into four components, each of which corresponds to one of the accessible values for the final angular momentum L. Substituting the explicit expression of the 3 – j symbols, one finds :

$$\frac{1}{I^{2}}\left(\frac{d\sigma}{d\Omega}\right)_{nlm}=\frac{\pi^{2}a_{0}^{2}\alpha\omega}{I_{0}^{2}}\left|M_{l+3}+M_{l+1}+M_{l-1}+M_{l-3}\right|^{2} \quad (2)$$

Where the expressions of the partial amplitudes M_L read (Maquet, 1977):

For linear polarization:

$$M_{l+3}=(-i)^{l+3}e^{i\delta_{l+3}}\left(\frac{\left[(l+1)^{2}-m^{2}\right]\left[(l+2)^{2}-m^{2}\right]\left[(l+3)^{2}-m^{2}\right]}{(2l+1)(2l+3)^{2}(2l+7)(2l+5)^{2}}\right)^{\frac{1}{2}}\times T_{l+1,l+2,l+3}Y_{1+3,m}(\hat{k}) \quad (3)$$

$$M_{l+1}=(-i)^{l+1}e^{i\delta_{l+1}}Y_{l+1,m}(\hat{k})\begin{pmatrix}\left(\frac{(l+1)^{2}-m^{2}}{(2l+1)(2l+3)}\right)^{\frac{3}{2}}T_{l+1,l,l+1}\\+\left(\frac{\left[(l+1)^{2}-m^{2}\right]\left[(l+2)^{2}-m^{2}\right]}{(2l+1)(2l+3)^{3}(2l+5)^{2}}\right)^{\frac{1}{2}}T_{l+1,l+2,l+1}\\+\left(\frac{\left[l^{2}-m^{2}\right]\left[(l+1)^{2}-m^{2}\right]}{(2l+1)^{3}(2l+3)(2l-1)^{2}}\right)^{\frac{1}{2}}T_{l-1,l,l+1}\end{pmatrix} \quad (4)$$

$$M_{l-1}=(-i)^{l-1}e^{i\delta_{l-1}}Y_{l-1;m}(\hat{k})\begin{pmatrix}\left(\frac{l^{2}-m^{2}}{(2l-1)(2l+1)}\right)^{\frac{3}{2}}T_{l-1,l,l-1,}\\+\left(\frac{\left[l^{2}-m^{2}\right]\left[(l-1)^{2}-m^{2}\right]}{(2l+1)(2l-1)^{3}(2l-3)^{2}}\right)^{\frac{1}{2}}T_{l-1,l-2,l-1}\\+\left(\frac{\left(l^{2}-m^{2}\right)\left[(l+1)^{2}-m^{2}\right]}{(2l-1)(2l+1)^{3}(2l+3)^{2}}\right)^{\frac{1}{2}}T_{l+1,l,l-1}\end{pmatrix} \quad (5)$$

$$M_{l-3}=(-i)^{l-3}e^{i\delta_{l-3}}\left(\frac{\left[(l-1)^{2}-m^{2}\right]\left[(l-2)^{2}-m^{2}\right]\left[(l^{2}-m^{2})\right]}{(2l+1)(2l-3)^{2}(2l-1)^{2}(2l-5)}\right)^{\frac{1}{2}}\times T_{l-1,l-2,l-3}Y_{l-3,m}(\hat{k}) \quad (6)$$

and for circularly polarized light:

$$M_{l+3}^{'}=(-i)^{l+3}e^{i\delta_{l+3}}Y_{l+3,m+3}\left(\hat{k}\right)T_{l+1,l+2,l+3}\times\left(\frac{(l+1+m)(l+2+m)(l+3+m(l+4+m)(l+5+m)(l+6+m))}{8(2l+1)(2l+3)^{2}(2l+5)^{2}(2l+7)}\right)^{\frac{1}{2}} \quad (7)$$

$$M_{l+1}=(-i)^{l+1}e^{i\delta_{l+1}}Y_{l+1,m+3}\left(\hat{k}\right)\times\left(\frac{(l+1+m)(l+2+m)(l+3+m)(l+4+m)(l-1+m)(l-m)}{8(2l+1)(2l+3)}\right)^{\frac{1}{2}}\times\left(\frac{T_{l-1,l,l+1}}{(2l-1)(2l+1)}+\frac{T_{l+1,l+2,l+1}}{(2l+5)(2l+3)}+\frac{T_{l+1,l,l+1}}{(2l+1)(2l+3)}\right) \quad (8)$$

$$M_{l-1}^{'}=(-i)^{l-1}e^{i\delta l-1}Y_{l-1,m+3}\left(\hat{k}\right)\times\left(\frac{(l+1+m)(l+2+m)(l-3-m)(l-2-m)(l-1-m)(l-m)}{8(2l+1)(2l+3)}\right)^{\frac{1}{2}}\times\left(\frac{T_{l-1,l,l-1}}{(2l-1)(2l+1)}+\frac{T_{l-1,l-2,l-1}}{(2l-1)(2l-3)}+\frac{T_{l+1,l,l-1}}{(2l+1)(2l+3)}\right) \quad (9)$$

$$M_{l-3}^{'}=\left(-i\right)^{l-3}e^{i\delta_{l}-3}Y_{l-3,m+3}\left(\hat{k}\right)T_{l-1,l-2,l-3}\times\left(\frac{(l-1-m)(l-2-m)(l-3-m)(l-4-m)(l-5-m)(l-m)}{8(2l+1)(2l-3)^{2}(2l-5)(2l-1)^{2}}\right)^{\frac{1}{2}} \quad (10)$$

Where,

$$T_{\lambda_1,\lambda_2,L}=\sum_{v}\frac{\left\langle R_{k,L}(r)\middle|r\middle|R_{v_2,\lambda_2}\right\rangle\left\langle R_{v_2,\lambda_2}\middle|R_{v_1\lambda_1}\middle|r\middle|R_{n,1}\right\rangle}{\left(E_{n,l}+2\omega-E_{v_2,\lambda_2}\right)\left(E_{n,l}+\omega-E_{v_1,\lambda_1}\right)}$$

is the radial transition matrix element.

Radial part

We recall briefly the method of the implicit summation technique, by applying it to the case of third order processes. The radial contribution $T_{\lambda_1,\lambda_2,L}$ due to the transition from the bound initial state (n, l, m) to the continuum final state (L, M) via intermediate states of orbital quantum numbers λ_1 and λ_2, is given by (Gontier et al., 1975):

$$T_{\lambda_1,\lambda_2,L} = (-1)^l \frac{1}{(2l+1)!}\left(\frac{(n+l)!}{(n-l-1)!(2n)}\right)^{\frac{1}{2}}\left(\frac{2}{n}\right)^{l+\frac{1}{2}}$$

$$\times\left({}_1F_1\left(-n+l+1;2l+2;-2p\frac{d}{dp}\right)\frac{d^{l-\lambda_1+2}}{dp^{l-\lambda_1+2}}y(\lambda_1,\lambda_2,L)\right)_{p=\frac{1}{n}} \quad (11)$$

Where the function y (λ_1, λ_2, L) is obtained by solving a set of first order inhomogeneous differential equations derived from the Schrodinger equation:

$$\left(\left(p^2-\alpha_2^2\right)\frac{d}{dp}+2(\lambda_2+1)p-1\right)y(\lambda_2,L) = -2\left(\frac{d}{dp}\right)^{\lambda_2-L+2} y_L \quad (12)$$

$$\left(\left(p^2-\alpha_1^2\right)\frac{d}{dp}+2(\lambda_1+1)p-1\right)y(\lambda_1,\lambda_2,L) = -2\left(\frac{d}{dp}\right)^{\lambda_1-\lambda_2+2} y(\lambda_2,L) \quad (13)$$

Where y_L is the (L+1)th derivative of the Laplace transform of the continuum radial function ; the quantities : $\alpha_q^2 = -2(q\omega + E_i)$, where E_i is the energy of the initial state. A particular value of y (λ_2, L) is obtained at the value p = α_2. In the case of ns states one must derive: T_{123}, T_{121} and T_{101}; while for np states there are: T_{234}, T_{232}, T_{212}, T_{210}, T_{012} and T_{010}. These contributing terms numerically evaluated, will allow us to arrive quantitatively at the angular coefficients given in linear and circular polarization.

RESULTS AND DISCUSSION

Analytical results

Linear polarisation

General formulas: We shall prove now that, although the θ dependence for the different magnetic sublevels is quite intricate indeed, containing power of cosθ as high as 2l + 6, the observed angular distribution will assume, for an unpolarized target, the simple form mentioned in the introductory part of this study, whatever the orbital quantum number, l. The angular distribution is now obtained by averaging over all magnetic sublevels assumed to be equally populated, then, Equation (2) yields:

$$\frac{1}{I^2}\frac{d\sigma_{n,l}}{d\Omega} = \frac{1}{2l+1}\sum_m \frac{1}{I^2}\frac{d\sigma_{n,l,m}}{d\Omega} \quad (14)$$

Using the well known formulas (Cooper and Zare, 1969)

$$\sum_m \left|Y_{l,m}\right|^2 = \frac{2l+1}{4\pi} \quad (15)$$

$$\sum_m m^2\left|Y_{l,m}\right|^2 = \frac{2l+1}{8\pi}l(l+1)\sin^2\theta \quad (16)$$

$$\sum_m m^4\left|Y_{l,m}\right|^2 = \frac{2l+1}{8\pi}l(l+1)\left(\sin^2\theta+\frac{3}{4}(l+2)(l-1)\sin^4\theta\right) \quad (17)$$

And establishing the summation formulas

$$\sum_m m^6\left|Y_{l,m}\right|^2 = \frac{2l+1}{8\pi}l(l+1)\left\{\sin^2\theta+\frac{15}{4}(l+2)(l-1)\sin^4\theta+\frac{5}{8}(l+2)(l+3)(l-1)(l-2)\sin^6\theta\right\} \quad (18)$$

Following to:

$$\sum_m m^6 = \frac{2l+1}{2l}l(l+1)\left(3l^4+6l^3-3l+1\right) \quad (19)$$

and summing term by term the corresponding explicit expressions of the angular coefficients, permits one to arrive at the general analytical results which are extremely lengthy and will not be shown here; the development of Equation (14) reads:

$$\frac{d\sigma_{n,l}}{I^2 d\Omega} = a + b\cos^2\theta + c\cos^4\theta + d\cos^6\theta \quad (20)$$

the distribution now has the form mentioned in the introductory part of this study.

For total cross sections calculations (Maquet, 1977), all the crossed terms $M_i M_j^*$ (i ≠ j) vanish owing to the orthogonality of the spherical harmonics; and, only subsist the quadratic terms. The existence of the crossed terms containing the phase shifts shows that the differential cross section is a more sensitive tool than the total cross section for testing theories. Nevertheless the total cross section can be indirectly deduced from Eq. (20), by expressing $\cos^2\theta$, $\cos^4\theta$ and $\cos^6\theta$ as a combination of Legendre polynomials of even order; one obtains:

$$\frac{d\sigma_{n,l}}{I^2 d\Omega} = A + BP_2(\cos\theta) + CP_4(\cos\theta) + DP_6(\cos\theta) \quad (21)$$

or

$$\frac{d\sigma_{n,l}}{I^2 d\Omega} = \frac{\sigma_{n,l}}{I^2 4\pi}\left(1+\beta_2 P_2(\cos\theta)+\beta_4 P_4(\cos\theta)+\beta_6 P_6(\cos\theta)\right)$$

Integrating this expression over the propagation direction of the ejected photo electron, allows one to get:

$$\frac{\sigma_{n,l}}{I^2} = 4\pi A \quad (22)$$

With:

$$A = a + \frac{b}{3} + \frac{c}{5} + \frac{d}{7}$$

In order to have an insight of these general expressions, we consider the particular cases of ns and np initial states.

Application to ns states: In this case, three channels are opened for the outgoing photoelectron:

1. s $\rightarrow$ p $\rightarrow$ d $\rightarrow$ kf
2. s $\rightarrow$ p $\rightarrow$ d $\rightarrow$ kp
3. s $\rightarrow$ p $\rightarrow$ s $\rightarrow$ kp

One easily gets the explicit expressions of the angular coefficients by substituting, l = 0 in all the above equations; then Equation (20) yields:

$$\frac{d\sigma_{n,0}}{I^2 d\Omega} = b\cos^2\theta + c\cos^4\theta + d\cos^6\theta \quad (23)$$

Where the isotropic term, a rigorously vanishes (a=0), and:

$$b = \frac{\pi\alpha\omega a_o^2}{4I_o^2}\left[\frac{9}{25}|T_{123}|^2 + \frac{1}{9}|T_{101}|^2 + \frac{16}{225}|T_{121}|^2 + \frac{8}{45}\mathrm{Re}\left(T_{101}T_{121}^*\right)\right.$$
$$\left. + \frac{2}{5}\mathrm{Re}\left(e^{i(\delta_3-\delta_1)}T_{123}T_{101}^*\right) + \frac{8}{25}\mathrm{Re}\left(e^{i(\delta_3-\delta_1)}T_{123}T_{121}^*\right)\right] \quad (24)$$

$$c = -\frac{\pi\alpha\omega a_o^2}{4I_o^2}\left[\frac{6}{5}|T_{123}|^2 + \frac{2}{3}\mathrm{Re}\left(e^{i(\delta_3-\delta_1)}T_{123}T_{101}^*\right)\right.$$
$$\left. + \frac{8}{25}\mathrm{Re}\left(e^{i(\delta_3-\delta_1)}T_{123}T_{121}^*\right)\right] \quad (25)$$

$$d = \frac{\pi\alpha\omega a_o^2}{4I_o^2}|T_{123}|^2 \quad (26)$$

We note that all the channels contribute to the weight of b and c coefficients while for d, only channel number 1 contributes; they interfere between them in b, whereas in c, the interference between the channels 2 and 3 does not occur. Equation (23) is different from that, found previously by Lambropoulos (1972), with the polarization vector lying in the (x, y) plane, implying a dependence of the distribution with ϕ (angle between the x-axis and a projection of the direction of the outgoing photoelectron), in addition to the θ angle. Unfortunately the corresponding explicit expressions of b, c and d coefficients are not yet given, to allow a comparison. With a zero isotropic term, this result is in full disagreement with the previous experimental ones (Fabre et al., 1981; Dodhy et al., 1986), showing a non zero isotropic term. As a test of our predictions from Equation (22), we deduce the corresponding total cross-section in conjunction with Equations (24), (25) and (26):

$$\frac{1}{I^2}\sigma_{ns} = \frac{\pi^2\alpha\omega a_0^2}{I_0^2}\left(\frac{4}{175}|T_{123}|^2 + \frac{1}{27}|T_{101}|^2 + \frac{16}{675}|T_{121}|^2 + \frac{8}{135}\mathrm{Re}\left(T_{101}T_{121}^*\right)\right) \quad (27)$$

This is same as that obtained earlier, directly by Maquet (1977).

The numerical values of the angular coefficients are displayed in the Tables 1(a), 2(a) and 3(a) for 1s, 2s, and 3s initial states; the corresponding curves are shown in Figures 1, 2(a) and 3(a). Following the same process, we consider the particular case of np initial states.

Application to np states: Occurrence of an isotropic term - In this case, six channels are allowed for the ejected photoelectron:

1'. p $\rightarrow$ d $\rightarrow$ f $\rightarrow$ kg
2'. p $\rightarrow$ d $\rightarrow$ p $\rightarrow$ kd
3'. p $\rightarrow$ d $\rightarrow$ f $\rightarrow$ kd
4'. p $\rightarrow$ d $\rightarrow$ p $\rightarrow$ ks
5'. p $\rightarrow$ s $\rightarrow$ p $\rightarrow$ kd
6'. p $\rightarrow$ s $\rightarrow$ p $\rightarrow$ ks

Substituting l = 1 in all equations, it comes for Equation (20):

$$\frac{d\sigma_{n,p}}{I^2 d\Omega} = a + b\cos^2\theta + c\cos^4\theta + d\cos^6\theta \quad (28)$$

Where:

$$a = \frac{\pi\alpha\omega a_0^2}{12I_0^2}\left(\frac{27}{5^2 7^2}|T_{234}|^2 + \frac{16}{3^3 5^2}|T_{210}|^2 + \frac{1}{3^3}|T_{010}|^2 + \frac{16}{3^3 5^2}|T_{212}|^2 + \frac{27}{5^2 7^2}|T_{232}|^2\right.$$
$$+ \frac{1}{27}|T_{012}|^2 + \frac{8}{3^3 5}\mathrm{Re}\left(T_{210}T_{010}^*\right) + \frac{2}{35}\mathrm{Re}\left(T_{232}T_{012}^*\right) + \frac{8}{5^2 7}\mathrm{Re}\left(T_{212}T_{232}^*\right)$$
$$+ \frac{8}{3^3 5}\mathrm{Re}\left(T_{212}T_{012}^*\right) + \frac{54}{5^2 7^2}\mathrm{Re}\left(e^{i(\delta_4-\delta_2)}T_{234}T_{232}^*\right) + \frac{2}{35}\mathrm{Re}\left(e^{i(\delta_4-\delta_2)}T_{234}T_{012}^*\right)$$
$$\left. + \frac{8}{5^2 7}R_e\left(e^{i'\delta_4-\delta_2)}T_{234}T_{212}^*\right) + \frac{8}{5^2 7}\mathrm{Re}\left(e^{i(\delta_4-\delta_0)}T_{234}T_{210}^*\right)\right.$$

Table 1. (a) Non resonant three photon ionization contributing coefficients ($cm^2\ w^{-2}\ sr^{-1}$); (b) the corresponding total cross-sections ($cm^6\ w^{-2}$) of H(1s): b, c, d and σ/I^2 for linearly polarized light; d' and σ'/I^2 for circularly polarized light.

(A) Angular coefficients

λ (nm)	b	c	d	d'
200	7.179 (-48)	-2.335 (- 47)	1.904 (-47)	2.380 (-48)
210	2.755 (-47)	-9.381 (-47)	8.142 (-47)	1.018 (-47)
220	2.006 (-47)	-6.637 (-47)	5.494(-47)	6.869 (-48)
229*	2.197 (-47)	-6.558 (-47)	5.340 (-47)	6.675 (-48)
230	2.264 (-47)	-6.558 (-47)	5.344 (-47)	6.680 (-48)
239*	9.221 (-47)	-5.615 (-47)	5.439 (-47)	6.799 (-48)
240	1.598 (-46)	-4.984 (-47)	5.451 (-47)	6.814 (-48)
244*	2.880 (-45)	-1.877 (-46)	5.495 (-47)	6.868 (-48)
248*	1.615 (-46)	-1.039 (-46)	5.523 (-47)	6.904 (-48)
250	1.870 (-46)	-9.998 (-47)	5.529 (-47)	6.912 (-48)
257*	6.515 (-47)	-9.866 (-47)	5.492 (-47)	6.864 (-48)
260	6.061 (-47)	-9.968 (-47)	5.440 (-47)	6.801 (-48)
264*	5.779 (-47)	-1.014 (-46)	5.334 (-47)	6.667 (-48)
270	5.665 (-47)	-1.039 (-46)	5.077 (-47)	6.347 (-48)
273.528	5.679 (-47)	-1.051 (-46)	4.866 (-47)	6.082 (-48)

(B) Total cross-sections

λ (nm)	Kristenko (1976)	Gao (1988)	(Radhakrishnan, 2004; Laplanche, 1976)			Present work	
	σ/I^2	σ'/I^2	σ/I^2	σ'/I^2	σ'/I^2	σ/I^2	σ'/I^2
200	5.577 (-48)	1.326 (-47)	5.423(-48)	1.324(-47)	1.365(-47)	5.570 (-48)	1.367 (-47)
210	2.582 (-47)	5.776 (-47)	2.539(-47)	5.772(-47)	5.771(-47)	2.580 (-47)	5.847 (-47)
220	1.590 (-47)	3.945 (-47)	1.588(-47)	3.943(-47)	3.957(-47)	1.589 (-47)	3.946 (-47)
229*	----------	----------				2.308 (-47)	3.835 (-47)
230	2.599 (-47)	3.840 (-47)	2.640(-47)	3.839(-47)	3.853(-47)	2.597 (-47)	3.838 (-47)
239*	----------	----------				3.427 (-46)	3.906 (-47)
240	6.422 (-46)	3.917 (-47)	7.056(-46)	3.917(-47)	3.935(-47)	6.488 (-46)	3.914 (-47)
244*	----------	----------				1.169 (-44)	3.946 (-47)
248*	----------	----------				5.145 (-46)	3.966 (-47)
250	3.034 (-46)	3.972 (-47)	2.948(-46)	3.972(-47)	3.998(-47)	3.032 (-46)	3.970 (-47)
257*	----------	----------				1.235 (-46)	3.943 (-47)
260	1.011 (-46)	3.906 (-47)	1.002(-46)	3.906(-47)	3.947(-47)	1.010 (-46)	3.907 (-47)

Table 1. Cont'd.

264*	----------	----------			8.304 (-47)	3.830 (-47)
270	----------	----------	6.705(-47)	3.641(-47)	6.732 (-47)	3.646 (-47)
273.528	----------	----------			6.100 (-47)	3.494 (-47)

* Corresponds to the second harmonic generation wavelength provided from an ion laser system based on Beta Borate (BBO) crystal; λ = 273.528 nm is the ionization threshold wavelength; the format A(n) means $A*10^n$.

Table 2. The same as in Table 1 but (A) for H(2s); B) for H(2p): Effect of the quantum orbital number; λ = 1094.112 nm, is the ionization threshold wavelength; a tunable titanium: Sapphire/Dye laser can provide wavelengths between 810 to 1000 nm; and 1060 nm by a CO_2 laser.

(A) 2s initial state

λ (nm)	b	c	d	d'	Present work		Maquet (1977)	
					σ/I^2	σ'/I^2	σ/I^2	σ'/I^2
810	9. 914 (-44)	-3. 074 (-43)	2. 438 (-43)	3. 047 (-44)	8 .270 (-44)	1. 751 (-43)	-	-
820	3 .260 (-40)	-1 .118 (-39)	9 .904 (-40)	1. 238 (-40)	3 .341 (-40)	7 .112 (-40)	-	-
830	3 .620 (-42)	-1 .242 (-41)	1 .081 (-41)	1 .351 (-42)	3 .348 (-42)	7 .763 (-42)	-	-
840	9 .480 (-43)	-3 .233 (-42)	2 .770 (-42)	3 .462 (-43)	8 .184 (-43)	1 .989 (-42)	-	-
860	1 .986 (42)	-6 .940 (-42)	6 .292 (-42)	7 .865 (-43)	2 .170 (-42)	4 .518 (-42)	-	-
870	2 .171 (-40)	-7 .561 (-40)	6 .691 (-40)	8 .364 (-41)	2 .103 (-40)	4 .805 (-40)	-	-
930	1 .891 (-43)	-6 .477 (-43)	5 .558 (-43)	6 .947 (-44)	1 .617 (-43)	3 .991 (-43)	-	-
940	7 .553 (-45)	-2 .746 (-44)	2 .571 (-44)	3 .214 (-45)	8 .700 (-45)	1 .846 (-44)	-	-
960	1 .061 (-41)	-3 .685 (-41)	3 .211 (-45)	4 .013 (-42)	9 .442 (-42)	2 .306 (-41)	-	-
970	5 .267 (-40)	-1 .828 (-39)	1 .590 (-39)	1 .987 (-40)	4 .660 (-40)	1 .142 (-39)	-	-
1 060	4 .783 (-42)	-1 .700 (-41)	1 .511 (-41)	1 .889 (-42)	4 .451 (-42)	1 .085 (-41)	-	-
1 094. 112	3 .532 (-42)	-1 .301 (-41)	1 .198 (-41)	1 .497 (-42)	3 .603 (-42)	8 .601 (-42)	3.600 (-42)	8.600 (-42)

(B) 2p initial state

λ (nm)	a	b	c	d	c'	d'	σ/I^2	σ'/I^2
810	2 .178 (-44)	6. 455 (-44)	-1 .051 (-43)	5 .604 (-44)	2 .563 (-44)	5. 599 (-45)	3. 806 (-43)	2 .039 (-43)
820	5 .334 (-36)	-4.235 (-36)	2.121 (-35)	3.313 (-40)	7.757 (-37)	-5.311 (-43)	1.026 (-34)	5.191 (-36)
830	1.485 (-43)	3.818 (-43)	-1.632 (-42)	1.987 (-42)	6.383 (-43)	2.428 (-43)	2.931 (-42)	5.673 (-42)
840	2.946 (-44)	2.090 (-43)	-5.486 (-43)	5.343 (-43)	1.760 (-43)	7.020 (-44)	8.260 (-43)	1.583 (-42)
850	5.490 (-45)	5.839 (-44)	-6.932 (-44)	2.565 (-44)	2.357 (-44)	7.660 (-45)	1.870 (-43)	2.020 (-43)
860	5.706 (-43)	4.901 (-42)	-4.897 (-42)	1.004 (-42)	3.524 (-43)	1.509 (-43)	1.719 (-41)	3.228 (-42)
870	4.197 (-37)	-4.568 (-37)	1.422 (-36)	3.670 (-39)	5.324 (-38)	-4.259 (-40)	6.939 (-36)	3.534 (-37)

Table 2. Cont'd.

900	6.708 (-44)	4.313 (-43)	-1.409 (-42)	1.514 (-42)	4.795 (-43)	1.808 (-43)	1.825 (-42)	4.253 (-42)
960	5.944 (-42)	2.870 (-41)	-4.188 (-42)	-1.444 (-42)	2.250 (-42)	2.661 (-42)	1.818 (40)	2.807 (-41)
970	3.819 (-36)	-2.233 (-36)	1.672 (-35)	-7.542 (-38)	5.933 (-37)	9.536 (-39)	8.052 (-35)	4.064 (-36)
980	1.130 (-39)	-1.461 (39)	2.272 (-39)	6.053 (-40)	2.029 (-40)	-5.376 (-41)	1.487 (-38)	1.051 (-39)
990	3.247 (-42)	7.727 (-42)	-3.619 (-41)	4.491 (-41)	1.065 (-41)	5.395 (-43)	6.285 (-41)	7.446 (-41)
1000	6.090 (-43)	5.825 (-42)	-2.061 (-41)	2.235 (-41)	5.576 (-42)	7.603 (-43)	2.039 (-41)	4.174 (-41)
1060	1.245 (-43)	2.417 (-42)	-8.786 (-42)	1.011 (-41)	2.359 (-42)	1.720 (-43)	7.765 (-42)	1.680 (-41)
1 094.112	4.961 (-44)	2.392 (-42)	-8.791 (-42)	1.041 (-41)	2.254 (-42)	-3.079 (-44)	7.242 (-42)	1.493 (-41)

Table 3. The same as in Table 2, but (A) for H(3s); (B) for H(3p). λ= 2461.752 nm is the ionization threshold wavelength; all the wavelengths can be obtained from a tunable Nd:YAG laser.

(A) 3s initial state

λ (nm)	b	c	d	d'	Present work		Maquet (1977)	
					σ/I^2	σ'/I^2	σ/I^2	σ'/I^2
1850	1. 245 (-36)	-4. 751 (-36)	4. 951 (-37)	6. 189 (-37)	2. 187 (-36)	3. 555 (-36)	-	-
1875	1. 759 (-35)	-5 .739 (-35)	4. 685 (-35)	5. 856 (-36)	1. 353 (-35)	3. 364 (-35)	-	-
1900	3. 385 (-37)	-1 .318 (-36)	1. 472 (-36)	1. 840 (-37)	7. 479 (-37)	1. 057 (-36)	-	-
1925	9. 898 (-38)	-3 .798 (-37)	3. 833 (-37)	4. 791 (-38)	1. 482 (-37)	2. 752 (-37)	-	-
1975	7. 470 (-40)	-2 .740 (-39)	4. 138 (-38)	5. 173 (-40)	3. 672 (-39)	2. 972 (-39)	-	-
2050	8 .704 (--39)	-3 .344 (-38)	3. 288 (-38)	4. 111 (-39)	1. 146 (-38)	2. 361 (-38)	-	-
2075	2 .375 (-39)	-8 .726 (-39)	8. 069 (-39)	1. 009 (-39)	2. 516 (-39)	5. 794 (-39)	-	-
2100	3 .907 (-40)	-1 .158 (-39)	8. 643 (-40)	1 .080 (-40)	2. 769 (-40)	6. 206 (-40)	-	-
2125	1 .704 (-40)	-7.441 (-40)	1. 190 (-39)	1 .488 (-40)	9. 803 (-40)	8. 547 (-40)	-	-
2200	1 .597 (-37)	-6 .492 (-37)	6. 755 (-37)	8 .444 (-38)	2. 502 (-37)	4. 851 (-37)	-	-
2225	2 .162 (-38)	-8 .656 (-38)	8. 810 (-38)	1 .101 (-38)	3. 116 (-38)	6. 326 (-38)	-	-
2420	3 .361 (-42)	-3 .151 (-41)	1. 201 (-40)	1 .501 (-41)	1. 505 (40)	8. 625 (-41)	-	-
2425	2 .107 (-41)	-1 .515 (-40)	2 .928 (-40)	3 .660 (-41)	2 .330 (-40)	2. 102 (-40)	-	-
2461.752	1 .100 (-39)	-5 .051 (-39)	5 .798 (-39)	7 .248 (-40)	2 .322 (-39)	4. 164 (-39)	2.320 (-39)	4.170 (-39)

(B) 3p initial state

λ (nm)	a	b	c	d	c'	d'	σ/I^2	σ'/I^2
1850	2 .161 (-33)	-2.782 (-33)	7. 373 (-33)	-6 .833 (-35)	2. 460 (-34)	8.829 (-36)	3 .391 (-32)	1. 699 (-33)
1900	3 .682 (-33)	-2 .225 (-33)	1.752 (-32)	6 .667 (-35)	6. 229 (-34)	-8. 248 (-36)	8.110 (-32)	4.127 (-33)
1925	3 .339 (-38)	6 .077 (-39)	-2. 484 (-38)	3 .500 (-38)	2 .650 (-38)	2 .012 (-38)	4. 454 (-37)	2 .932 (-37)
1975	9 .389 (-37)	-3 .668 (-37)	5 .778 (-36)	7 .047 (-38)	2 .053 (-37)	-8 .591 (-39)	2 .491 (-35)	1. 327 (-36)

Table 3. Cont'd.

2025	1 .993 (-37)	-3 .355 (-37)	6 .230 (-37)	-1 .167 (-37)	1 .692 (-38)	3 .160 (-38)	2 .455 (-36)	2 .960 (-37)
2050	9 .298 (-40)	9 .310 (-40)	-6 .206 (-39)	7 .249 (-39)	2 .830 (-39)	1 .472 (-39)	1 .300 (-38)	2.742 (-38)
2075	9 .339 (-40)	-1 .662 (-39)	5 .436 (-39)	-2 .221 (-39)	5 .167 (-40)	8 .984 (-40)	1 .445 (-38)	8 .624 (-39)
2150	1 .987 (-36)	-1 .005 (-36)	1 .194 (-35)	3 .526 (-37)	4 .403 (-37)	-4 .260 (-38)	5. 141 (-35)	2 .706 (-36)
2175	1 .785 (-33)	-1 .268 (-33)	8 .178 (-33)	4 .127 (-35)	2 .911 (-34)	-5 .131 (-36)	3 .775 (-32)	1 .921 (-33)
2250	6 .728 (-40)	1 .895 (-39)	-1 .014 (-38)	1 .302 (-38)	3 .967 (-39)	1 .372 (-39)	1. 429 (-38)	3 .447 (-38)
2300	2 .754 (-40)	1 .496 (-40)	-9 .117 (-40)	1 .564 (-39)	1 .027 (-39)	7 .851 (-40)	4 .603 (-39)	1 .138 (-38)
2325	2 .752 (-40)	8 .944 (-42)	1 .161 (-39)	-1 .095 (-39)	4 .430 (-40)	7 .185 (-40)	4. 447 (-39)	7 .096 (-39)
2350	3 .971 (-40)	-4 .241 (-40)	4 .157 (-39)	-2 .735 (-39)	1 .216 (-40)	6 .542 (-40)	8 .751 (-39)	4 .573 (-39)
2461.752	1 .164 (-38)	-3 .443 (-38)	3 .168 (-38)	8 .399 (-39)	1 .644 (-39)	-8 .216 (-40)	9 .682 (-38)	6 .295 (-39)

$$+\frac{2}{35}\mathrm{Re}\left(e^{i(\delta_4-\delta_0)}T_{234}T_{010}^{*}\right)+\frac{32}{3^3 5^2}\mathrm{Re}\left(e^{i(\delta_2-\delta_0)}T_{212}T_{210}^{*}\right)$$

$$+\frac{8}{5^2 7}\mathrm{Re}\left(e^{i(\delta_2-\delta_0)}T_{232}T_{210}^{*}\right)+\frac{2}{35}\mathrm{Re}\left(e^{i(\delta_2-\delta_0)}T_{232}T_{010}^{*}\right)$$

$$+\frac{2}{3^3}\mathrm{Re}\left(e^{i(\delta_2-\delta_0)}T_{012}T_{010}^{*}\right)+\frac{4}{3^3 5}\mathrm{Re}\left(e^{i(\delta_2-\delta_0)}T_{012}T_{210}^{*}\right)$$

$$+\frac{4}{3^3 5}\mathrm{Re}\left(e^{i(\delta_2-\delta_0)}T_{212}T_{010}^{*}\right)\Bigg] \quad (29)$$

$$b=-\frac{\pi\alpha\omega a_O^2}{12I_0^2}\left(\frac{-27}{7^2 5}|T_{234}|^2+\frac{1}{45}|T_{212}|^2-\frac{6}{7^2 5}|T_{232}|^2+\frac{2}{9}|T_{012}|^2\right.$$

$$+\frac{12}{35}\mathrm{Re}\left(T_{232}T_{012}^{*}\right)+\frac{16}{45}\mathrm{Re}\left(T_{212}T_{012}^{*}\right)-\frac{18}{5^2 7^2}\mathrm{Re}\left(e^{i(\delta_4-\delta_2)}T_{234}T_{232}^{*}\right)$$

$$+\frac{26}{35}\mathrm{Re}\left(e^{i(\delta_4-\delta_2)}T_{234}T_{012}^{*}\right)+\frac{2}{5^2}\mathrm{Re}\left(e^{i(\delta_4-\delta_2)}T_{234}T_{212}^{*}\right)$$

$$+\frac{4}{7}\mathrm{Re}\left(e^{i(\delta_4-\delta_0)}T_{234}T_{010}^{*}\right)+\frac{32}{3^2 5^2}\mathrm{Re}\left(e^{i(\delta_2-\delta_0)}T_{212}T_{210}^{*}\right)$$

$$+\frac{24}{5^2 7}\mathrm{Re}\left(e^{i(\delta_2-\delta_0)}T_{232}T_{210}^{*}\right)-\frac{4}{45}\mathrm{Re}\left(e^{i(\delta_4-\delta_0)}T_{012}T_{010}^{*}\right)$$

$$+\frac{6}{35}\mathrm{Re}\left(e^{i(\delta_2-\delta_0)}T_{232}T_{010}^{*}\right)-\frac{16}{5^2 3^2}\mathrm{Re}\left(e^{i(\delta_2-\delta_0)}T_{212}T_{010}^{*}\right)$$

$$-\frac{16}{5^2 3^2}\mathrm{Re}\left(e^{i(\delta_2-\delta_0)}T_{012}T_{210}^{*}\right)+\frac{16}{35}\mathrm{Re}\left(e^{i(\delta_4-\delta_0)}T_{234}T_{210}^{*}\right) \quad (30)$$

$$c=\frac{\pi\alpha\omega a_O^2}{12I_0^2}\left(-\frac{99}{7^2 5}|T_{234}|^2+\frac{7}{5^2 3}|T_{212}|^2+\frac{51}{7^2 5^2}|T_{232}|^2\right.$$

$$+\frac{1}{3}|T_{012}|^2+\frac{36}{70}\mathrm{Re}(T_{232}T_{012}^{*})+\frac{24}{5^2 7}\mathrm{Re}(T_{212}T_{232}^{*})+\frac{8}{15}\mathrm{Re}(T_{212}T_{012}^{*})$$

$$-\frac{6}{7^2}\mathrm{Re}\left(e^{i(\delta_4-\delta_2)}T_{234}T_{232}^{*}\right)+\frac{50}{21}\mathrm{Re}\left(e^{i(\delta_4-\delta_2)}T_{234}T_{012}^{*}\right)$$

$$+\frac{4}{21}\mathrm{Re}\left(e^{i(\delta_4-\delta_2)}T_{234}T_{212}^{*}\right)+\frac{8}{15}\mathrm{Re}\left(e^{i(\delta_4-\delta_0)}T_{234}T_{210}^{*}\right)$$

$$+\frac{2}{3}\mathrm{Re}\left(e^{i(\delta_4-\delta_0)}T_{234}T_{010}^{*}\right)-\frac{4}{15}\mathrm{Re}\left(e^{i(\delta_2-\delta_0)}T_{212}T_{210}^{*}\right)$$

$$-\frac{4}{15}\mathrm{Re}\left(e^{i(\delta_2-\delta_0)}T_{012}T_{210}^{*}\right)-\frac{1}{3}\mathrm{Re}\left(e^{i(\delta_2-\delta_0)}T_{012}T_{010}^{*}\right)\Bigg) \quad (31)$$

$$d=\frac{\pi\alpha\omega a_O^2}{12I_0^2}\left(\frac{3}{7}|T_{234}|^2-\frac{6}{35}\mathrm{Re}\left(e^{i(\delta_4-\delta_2)}T_{234}T_{232}^{*}\right)\right.$$

$$-2\,\mathrm{Re}\left(e^{i\delta_4-\delta_2)}T_{234}T_{012}^{*}\right)-\frac{2}{5}\mathrm{Re}\left(e^{i(\delta_4-\delta_2)}T_{234}T_{212}^{*}\right)\Bigg) \quad (32)$$

In contrast with ns initial states, the distribution here, is marked by the occurrence of an isotropic term, a. As a consequence of the number of allowed channels, the number of terms increases to reach twenty-one terms for a, seventeen for b, fifteen for c, and four for d; obviously, the number of interference terms also increases; however, channels 5' and 6' do not contribute in d weight. These analytical expressions would be, to our knowledge the first to be reported, even if, that of the total cross sections do exist (Maquet 1977).

As a test of our predictions, taking into account Equation (22), together with Equations (29) - (32), one finds for the total cross-section:

$$\frac{\sigma_{n,p}}{I^2}=\frac{\pi\alpha\omega\, a_O^2}{105\, I_0^2}\left(\frac{144}{105}|T_{234}|^2+\frac{826}{675}|T_{212}|^2+\frac{708}{525}|T_{234}|^2+\frac{28}{27}|T_{012}|^2+\frac{35}{27}|T_{010}|^2\right.$$

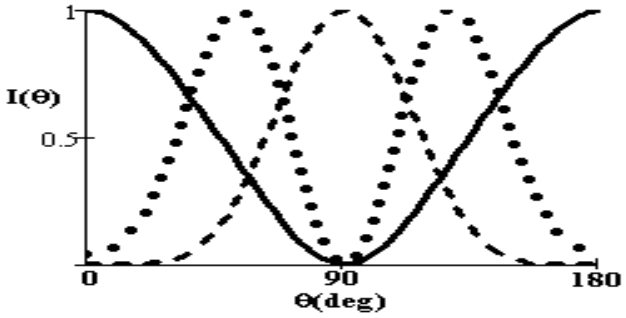

Figure 1. Normalized photoelectron angular distribution from non resonant three photons Ionization of hydrogen atom initially in its fundamental state: linear polarization :λ = 250 nm (full line); λ = 273.528 nm (dotted line); circular polarization: λ = 250 nm (dashed line).

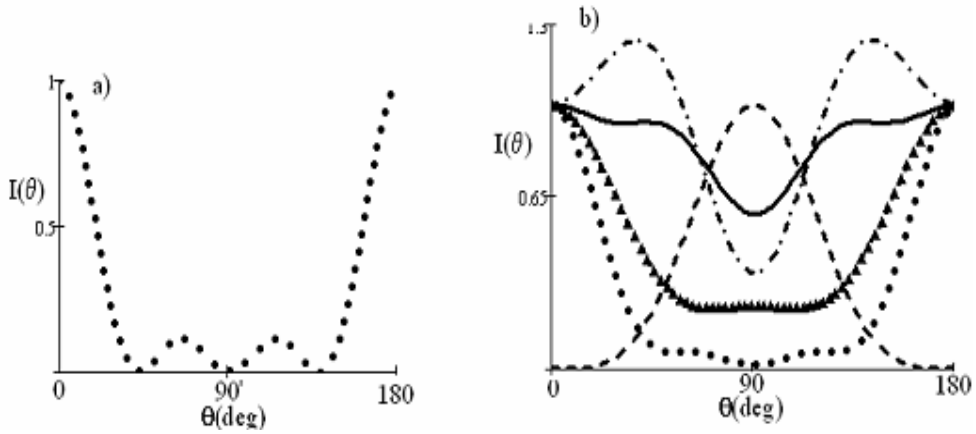

Figure 2. Quantum orbital effect in normalized photoelectron angular distribution from non resonant three photons ionization of H initially in n = 2,state: linear polarization: a)for 2s state, λ = 1094.112 nm ; b) for 2p state, λ = 810 nm (full line), λ = 820 nm (full triangle line), λ = 860 nm (chain line), $\lambda_{threshold}$ = 1094.112 nm (dotted line); circular polarization: λ = 860 nm (dashed line).

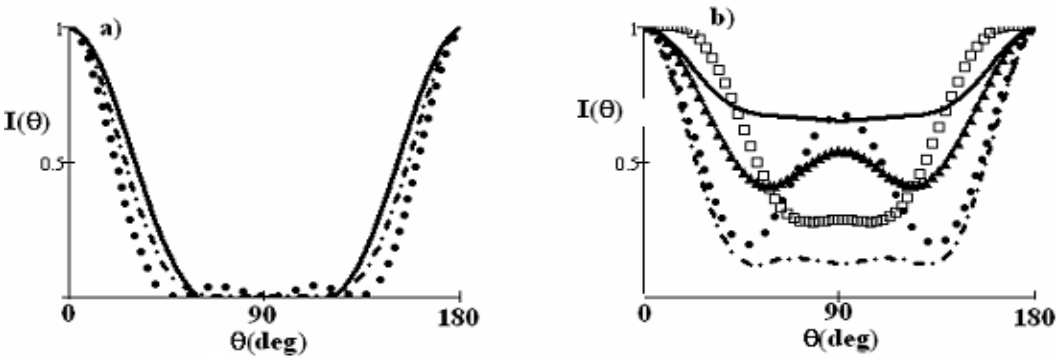

Figure 3. The same as in fig 2, but for H in its n=3 state, and for linear polarization only: for 3s state: λ = 1850 nm (full line), λ = 2420 nm (chain line), λ = 2461.752 nm (dotted line); b) 3p state: λ = 1925 nm (full line), λ = 2025 nm (full triangle line), λ = 2250 nm (chain line), λ = 2350 nm (square line), λ = 2461.752 nm (dotted line).

$$+\frac{112}{135}|T_{210}|^2+\frac{224}{135}\mathrm{Re}(T_{232}T_{012}^*)+\frac{576}{225}\mathrm{Re}(T_{212}T_{232}^*)+\frac{72}{45}\mathrm{Re}(T_{012}T_{232}^*)+\frac{56}{27}\mathrm{Re}\left(T_{010}T_{210}^*\right)\Bigg) \quad (33)$$

This is identical to that obtained by Maquet (1977). The numerical results are shown in the Tables 2(b) and 3(b), for 2p and 3p states, and some corresponding curves are displayed in Figures 2(b) and 3(b).

We establish now for any initial state of quantum numbers n and l, the general expressions of the angular distribution in the case of circularly polarized light.

Circularly polarized light

General formulas: Taking into account Equations (15) - (18), and summing the term by the corresponding explicit expressions of the angular coefficients, permits one to arrive at the general analytical results which are extremely lengthy and will not be shown here; the development of Equation (14) yields a sine form as mentioned in the introductory part of this study:

$$\frac{d\sigma_{n,l}^{'}}{I^2\cdot d\Omega}=a^{'}+b^{'}\cdot\sin^2\theta+c^{'}\sin^4\theta+d^{'}\sin^6\theta \quad (34)$$

Independent of the ϕ angle; here, θ is the angle between the direction of light propagation and that of the emitted photoelectron. In order to have an insight into these general expressions, we consider the particular cases of ns, and np states.

Application to ns initial states: In this case, one easily gets the expressions only by substituting l=0 in all the equations, then Equation (34) yields:

$a^{'}=0$; $b^{'}=0$; $c^{'}=0$; rigorously,

So

$$\frac{d\sigma_{n,s}^{'}}{I^2\cdot d\Omega}=d^{'}\sin^6\theta \quad (35)$$

With

$$d^{'}=\frac{\pi\,\alpha\,\omega\,a_0^2}{32\;I_0^2}\cdot|T_{123}|^2$$

This form is a particular case of that established earlier by Klarsfeld and Maquet (1972), for N photon ionization. From the explicit expression of d, in Eq.(26), one obtains:

$$d^{'}=\frac{d}{8}$$

$$\frac{\sigma_{ns}^{'}}{I_0^2}=\frac{8\pi d}{35} \quad (36)$$

We note that, only the channel 1, appearing in the case of ns states, for linearly polarized light, is allowed, since for right-hand (left-hand) circularly polarized light, the channels 2 and 3 are forbidden by the selection rules: $\Delta m=\pm1$

The numerical results for 1s, 2s and 3s states are shown in the Tables 1(a), 2(a) and 3(a), one corresponding curve is displayed in Figure 1. Even if most of the works (Gontier et al., 1986) have been done for ns initial states, it would seem of particular theoretical interest to treat the case where np initial states are considered, in comparison with the analytical results obtained for linearly polarized light treated in (Application to np states: Occurrence of an isotropic term).

Application to np initial states

Substituting l=1 in all the above equations, a' and b' rigorously vanish; so Equation (34) reads:

$$\frac{1}{I^2}\frac{d\sigma_{n,p}^{'}}{d\Omega}=c^{'}\sin^4\theta+d^{'}\sin^6\theta \quad (37)$$

With

$$c^{'}=\frac{\pi\alpha\omega a_0^2}{12I_0^2}\cdot\left(\frac{27}{196}|T_{234}|^2+\frac{3}{4}\left|\frac{T_{012}}{3}+\frac{T_{232}}{35}+\frac{T_{212}}{15}\right|^2-\frac{9}{14}\mathrm{Re}\left(e^{i(\delta_4-\delta_2)}T_{234}\left(\frac{T_{012}^*}{3}+\frac{T_{232}^*}{35}+\frac{T_{212}^*}{15}\right)\right)\right) \quad (38)$$

$$d^{'}=\frac{\pi\alpha\omega a_0^2}{12I_0^2}\cdot\left(\frac{3}{56}|T_{234}|^2+\frac{3}{4}\mathrm{Re}\left(e^{i(\delta_4-\delta_2)}T_{234}\left(\frac{T_{012}^*}{3}+\frac{T_{232}^*}{35}+\frac{T_{212}^*}{15}\right)\right)\right) \quad (39)$$

These expressions would to our knowledge, be the first to be reported. We note that like the d coefficient obtained for linearly polarized light, channels 4' and 6' are closed. As a consequence, great simplifications would occur in their interpretations. As a test of our predictions, taking into account Equation (22) in its equivalent form that is,

$$A^{'}=4\pi\left(a^{'}+\frac{2b^{'}}{3}+\frac{8c^{'}}{15}+\frac{16d^{'}}{35}\right) \quad (40)$$

The corresponding total cross section reads:

$$\frac{\sigma_{n,p}^{'}}{I^2}=\frac{\pi^2\alpha\omega a_0^2}{I_0^2}\cdot\left(\frac{8}{245}\cdot|T_{234}|^2+\frac{2}{15}\cdot\left|\frac{T_{012}}{3}+\frac{T_{232}}{35}+\frac{T_{212}}{15}\right|^2\right) \quad (41)$$

This is exactly the same as that established earlier by Maquet (1977).

Numerical values are shown in the Tables 2(b) and 3(b), for 2p and 3p states, and one corresponding curve displayed in Figure 2(b).

In order to have reliable insights about the behaviour of the differential cross section, we make a quantitative analysis of the problem. Various wavelengths including the ionization threshold are considered.

Numerical calculations

Series solutions of Equations (12) and (13)

As expressed in the radial part of the work, we give below, the explicit expressions of, $y(\lambda_2;L)$, y_L and $y(\lambda_1,\lambda_2;L)$ functions, of Equations (12) and (13), needed for the determination of the contributing radial matrix elements $T_{\lambda_1,\lambda_2,L}$.

From the second member of Equation (12), the Laplace transform of the well known hydrogenic function R_{kL} (Zernik and Klopfenstein, 1965), reads:

$$y_L = \int_0^\infty r^{L+1} R_{kL}(r) e^{-pr} dr = A_L \cdot G_L(p,k) \quad (42)$$

With

$$A_L(k) = \frac{(-2)^{L+1}}{\left(1-e^{-\frac{2\pi}{k}}\right)^{1/2}} \cdot \left[(1+k^2)(1+4k^2)\cdots(1+L^2k^2)\right]^{1/2}$$

and $G_L(p,k) = \dfrac{e^{-\frac{2}{k}arc\cot g\left(\frac{p}{k}\right)}}{\left(p^2+k^2\right)^{L+1}}$ (43)

We write:

$$F_{\lambda_2,L}(p;k) = 2A_L(k)\left(\frac{d}{dp}\right)^{\lambda_2-L+2} G_L(p,k) \quad (44)$$

One differentiates Equation (43) with respect to *p* to obtain:

$$G_L^{(1)}(p,k) = \frac{2(1-(L+1)p)}{p^2+k^2} \cdot G_L(p,k) \quad (45)$$

Continued differentiation of Equation (43) leads to the general relation:

$$(p^2+k^2)G_L^{(n+1)} = 2[1-(L+1+n)p]G_L^{(n)} - n(2L+1+n)G_L^{(n-1)} \quad (46)$$

$G_L^{(n)}$ is the n-th derivative of G_L.

An arbitrary point p_0 in the real plan is considered, the real variable x is defined as:

$$x = p - p_0;$$

and the Taylor series for:

$$y(\lambda_2,L) = \sum_n a_n x^n \quad (47)$$

$$F_{\lambda_2,L}(p,k) = \sum_n b_n x^n \quad (48)$$

And

$$y(\lambda_1,\lambda_2,L) = \sum_n c_n x^n \quad (49)$$

Determination of the b_n coefficients: From the selection rules we distinguish two cases from Equation (44)

.) $L = \lambda_2 + 1$; and **..)** $L = \lambda_2 - 1$

When **.)** is considered, one obtains the Taylor development of $F_{\lambda_2,L}$ around $p_0 (= \alpha_1 \text{ and } \alpha_2)$

$$F_{\lambda_2,L}(p,k) = A_L(k) \cdot G_L^{(1)} = A_L \sum_n \frac{G_L^{(n+1)}(p_0)}{n!} \cdot x^n \quad (50)$$

In comparison with Equation (48), this gives:

$$b_n = A_L \cdot \frac{G_L^{(n+1)}(p_0)}{n!} \quad (51)$$

Taking into account Equation (46), the recurrence relations between b_{n+1}, b_n and b_{n-1}, yields:

$$b_{n+1} = \frac{1}{p_0^2+k^2}\left\{\frac{2[1-(L+2+n)p_0]b_n}{n+1} - \frac{2L+2+n}{n} b_{n-1}\right\} \quad (52)$$

Where: $b_0 = A_L(k) \cdot G_L^{(1)}(p_0)$ and $b_1 = A_L \cdot G_L^{(2)}(p_0)$

When case **..)** is considered, then:

$$F_{\lambda_2,L}(p;k) = A_L \cdot G_L^{(3)} = A_L \sum_n \frac{G_L^{(n+3)}(p_0)}{n!} x^n \quad (53)$$

And

$$b_n = A_L \frac{G_L^{(n+3)}(p_0)}{n!} \quad (54)$$

Where: $b_0 = A_L(k) \cdot G_L^{(3)}(p_0)$ and $b_1 = A_L \cdot G_L^{(4)}(p_0)$

The recursive relations read now:

$$b_{n+1} = \frac{1}{p_0^2 + k^2}\left\{\frac{2[1-(L+4+n)p_0]b_n}{n+1} - \frac{(n+3)(2L+4+n)}{n(n+1)} b_{n-1}\right\} \quad (55)$$

Determination of the c_n coefficients: We consider the point $p_0 = \alpha_1$ in the real plan, and we define a variable $x = p - \alpha_1$; by substituting Equations (47) and (49) into Equation (13), and taking into account the case when:

$\lambda_1 = \lambda_2 + 1$;

one obtains:

$$\sum_{n=2}\{(n+1+2\lambda_1)c_{n-1} + 2[(n+1+\lambda_1)\alpha_1 - 1]c_n + 2(n+1)a_{n+1}\}x^n + \{2(\lambda_1+1)c_0 + 2[(\lambda_1+2)\alpha_1 - 1]c_1 + 4a_2\}x + 2[(\lambda_1+1)\alpha_1 - 1]c_0 + 2a_1 = 0 \quad (56)$$

$$c_n = -\frac{2(n+1)a_{n+1} + (n+1+2\lambda_1)c_{n-1}}{2[(n+1+\lambda_1)\alpha_1 - 1]} \quad (56')$$

And

$$c_0 = -\frac{a_1}{(\lambda_1+1)\alpha_1 - 1}$$

While for ii): $\lambda_2 = \lambda_1 - 1$;

One obtains:

$$\sum_{n=2}\{(n+1+2\lambda_1)c_{n-1} + 2[(n+1+\lambda_1)\alpha_1 - 1]c_n + 2(n+1)(n+2)(n+3)a_{n+3}\}x^n + \{2(\lambda_1+1)c_0 + 2[(\lambda_1+2)\alpha_1 - 1]c_1 + 2\times2\times3\times4a_4\}x + 2[(\lambda_1+1)\alpha_1 - 1]c_0 + 2\times6a_3 = 0 \quad (57)$$

This yields:

$$c_n = -\frac{2(n+1)(n+2)(n+3)a_{n+3} + (n+1+2\lambda_1)c_{n-1}}{2[(n+1+\lambda_1)\alpha_1 - 1]} \quad (58)$$

and

$$c_0 = -\frac{6a_3}{(\lambda_1+1)\alpha_1 - 1}$$

Determination of the a_n coefficients: Substituting Equations (47) and (48) into Equation (12), leads to:

$$\sum_{n=2}\{(p_0^2 - \alpha_2^2)(n+1)a_{n+1} + 2[(n+1+\lambda_2)\alpha_2 - 1]a_n + (n+1+2\lambda_2)a_{n-1} - 2b_n\}x^n + \{2p_0a_1 + 2(p_0^2 - \alpha_2^2)a_2 + 2(\lambda_2+1)a_0 + 2[(\lambda_2+1)p_0 - 1]a_1 - 2b_1\}x + \{(p_0^2 - \alpha_2^2)a_1 + 2[(\lambda_2+1)p_0 - 1]a_0 - 2b_0\} = 0 \quad (59)$$

Hence, when $p_0 = \alpha_2$:

$$a_0 = \frac{b_0}{(\lambda_2+1)\alpha_2 - 1}$$

$$a_{n+1} = \frac{2b_{n+1} - (n+1+2\lambda_2)a_n}{2[(n+2+\lambda_2)\alpha_2 - 1]} \quad (60)$$

$$n \geq 0$$

While when $p_0 = \alpha_1$, one obtains:

$$a_0 = y_{\alpha_1}(\lambda_2, L) = \sum_n a_n(\alpha_1 - \alpha_2)^n \quad (61)$$

Where the a_n are given by Equation (60);

$$a_1 = \frac{2b_0 - 2[(1+\lambda_2)\alpha_1 - 1]a_0}{(\alpha_1^2 - \alpha_2^2)} \quad (62)$$

and

$$a_{n+1} = \frac{2b_n - 2a_n[(n+1+\lambda_2)\alpha_1 - 1] - (2\lambda_2 + n + 1)a_{n-1}}{\alpha_1^2 - \alpha_2^2} \quad (63)$$

$$n \geq 1$$

The coefficients of the Taylor series are hence recursively determined and we can now calculate the general expressions of $T_{\lambda_1,\lambda_2,L}$ given by Equation (11).

General expressions of $T_{\lambda_1,\lambda_2,L}$

From Equation (11), two cases occur: i) $\lambda_1 = l+1$ and ii) $\lambda_1 = l-1$;

Thus, if i) is considered:

$$\left(\frac{d}{dp}\right)^{\lambda_1} y(\lambda_1, \lambda_2, L) = \sum_{n=1} nc_n x^{n-1} \quad (64)$$

While for ii), one obtains:

$$\left(\frac{d}{dp}\right)^3 y(\lambda_1,\lambda_2 L)=\sum_{n=3} n(n-1)(n-2)c_n x^{n-3} \quad (65)$$

These expressions, in conjunction with the well known development of the confluent hypergeometric function:

$${}_1F_1(\alpha,\beta,z)=1+\frac{\alpha}{\beta}z+\frac{\alpha(\alpha+1)}{\beta(\beta+1)}\frac{z^2}{2!}+\ldots+ \quad (66)$$

permits us to arrive at the general form of $T_{\lambda_1,\lambda_2,L}$ for the different initial states that is: 1s, 2s, 3s, 2p and 3p.

Fundamental state: n=1; l=0; λ_1=1; x=1-α_1

$$T_{1,\lambda_2,L}=2\sum_{n=1} nc_n x^{n-1} \quad (67)$$

2s metastable state: n=2; l=0; λ_1=1; $x=\frac{1}{2}-\alpha_1$

$$T_{1,\lambda_2,L}=\frac{1}{\sqrt{2}}\left\{\sum_{n=1} nc_n x^{n-1}+\frac{1}{2}\sum_{n=2} n(n-1)c_n x^{n-2}\right\} \quad (68)$$

3s initial state: n=3; l=0; λ_1=1; $x=\frac{1}{3}-\alpha_1$

$$T_{1,\lambda_2,L}=\frac{2}{3\sqrt{3}}\left\{\sum_{n=1} nc_n x^{n-1}+\frac{2}{3}\sum_{n=2} n(n-1)c_n x^{n-2}+\frac{2}{27}\sum_{n=3} n(n-1)(n-2)c_n x^{n-3}\right\} \quad (69)$$

T_{123}, T_{121} and T_{101}, needed for the angular coefficients calculations (Application to ns states) for these states, have the same above forms.

2p initial state: n=2; l=1; λ_1=0 or λ_1=2; $x=\frac{1}{2}-\alpha_1$

$$T_{0,\lambda_2,L}=\frac{1}{2\sqrt{6}}\sum_{n=3} n(n-1)(n-2)c_n x^{n-3} \quad (70)$$

$$T_{2,\lambda_2,L}=-\frac{1}{2\sqrt{6}}\sum_{n=1} nc_n x^{n-1} \quad (71)$$

3p initial state: n=3, l=1, λ_1=0 or λ_1=2; $x=\frac{1}{3}-\alpha_1$

$$T_{0,\lambda_2,L}=-\frac{2^2}{3^3}\sqrt{\frac{2}{3}}\left\{\sum_{n=3} n(n-1)(n-2)c_n x^{n-3}+\frac{1}{6}\sum_{n=4} n(n-1)(n-2)(n-3)c_n x^{n-4}\right\} \quad (72)$$

$$T_{2,\lambda_2,L}=-\frac{2^2}{3^3}\sqrt{\frac{2}{3}}\left\{\sum_{n=1} nc_n x^{n-1}+\frac{1}{6}\sum_{n=2} n(n-1)c_n x^{n-2}\right\} \quad (73)$$

T_{012} and T_{010} needed for the angular coefficients calculations (Application to np states: Occurrence of an isotropic term), have the same forms than Equations (70) and (72); while T_{234}, T_{232} and T_{210} have the same forms than Equations (71) and (73).

We can now discuss these results.

Linear polarization

Fundamental state: Table 1 displays the numerical values of the angular coefficients b, c and d ($cm^6.W^{-2}.sr^{-1}$) in a), and the corresponding total cross sections $\frac{\sigma_{n,l}}{I^2}$ ($cm^6.W^{-2}$), in b) for a wide range of wavelengths including second harmonic generation provided from an ion laser system based on Beta Barium Borate crystal. Since the c coefficient is always negative, it would mean that, from its explicit expression of Equation (25), the interference terms between channels 1 – 2 and between 1 – 3 are either constructive or destructive; in this last case, the quadratic term will always be more weighted.

It is noted in Figure 1, that maximum distribution is obtained for λ = 250 nm (full line) in the laser polarization direction, while for $\lambda_{threshold}$ = 273.528 nm (dotted line), it is located at θ = 54° (125°). Figure 1 also predicts zero distribution at θ = 90°, in agreement with that obtained by Potvliege and Shakeshaft (1988), who used non perturbative calculations; but, in disagreement with that observed from Cesium atom by Dodhy et al. (1985), which showed a departure from zero; Lambropoulos and Tang (1986) attributed that feature to spin-orbit coupling in the continuum; Furthermore, our calculated total cross sections in Table 1b) agree globally well with previous calculations using Sturmian expansion (Maquet, 1977; Kristenko and Vetchinkin, 1976; Laplanche et al., 1976) or variational method (Gao and Starace, 1988).

2s and 2p states: Table 2a) reveals again for 2s, a negative sign for c, while in b) for 2p, b, c and d are either positive or negative. These signs depend on how the contributing terms of their explicit expressions found in Application to np states: Occurrence of an isotropic term, compete between them; the same remark holds for the weight of the isotropic term, a which can take either a relatively high value as in Figure 2b) for λ = 810 nm (full line), or a nearly zero value for $\lambda_{threshold}$ = 1094.112 nm (dotted line). Based on the above, the fifteen interference terms of Equation (38) between channels 1' and 2' are strongly destructive and nearly swept the other constructive terms, yielding a very small value for a. We note also that the shapes are very sensitive to small

wavelengths change as shown in Figures 2b) for λ = 810 nm (full line), 820 nm (full triangle line) and 860 nm (chain line). In addition to these contrasts, the chain line curve (λ = 860 nm), shows a shallow minimum value around θ = 0° (180°) where only channel 2' occurs in the final state. Another feature to be noted is that, the triangle line curve (λ = 820 nm) follows: $a + b\cos^2\theta + c\cos^4\theta$ behaviour, recalling the second order processes. A similar shape as in Figure 2a) λ = 1094.112 nm, has been obtained from Lithium atom by Chen and Robicheaux (1996), who used an R-matrix Floquet calculations.

For total cross-sections and at threshold, our results in Table 2a), agree well for 2s state with that of Maquet (1977). Apart this wavelength, there would be no available calculated data as for Table 1b), although most mentioned wavelengths can be provided from tunable Titanium: Sapphire/Dye laser (810 to 1000 nm) and CO_2 laser (1060 nm) to permit further comparisons with experimental data.

3s and 3p initial states: All the wavelengths mentioned in Table 3 can be obtained from a tunable Nd : Yag laser. Same remarks above made about the signs and weights of the different coefficients in Table 2, apply here; as a consequence, all the displayed curves in Figure 3 are much contrasted, even if the distributions are always peaked in the laser polarization direction. However the square line curve (λ = 2350 nm) in Figure 3b), reveals an interesting feature, the maximum is nearly constant between θ = 0° and 30°; the same behaviour is observed for the minimum around θ = 90°. One can also see that in the Figure 3a), the dotted line curve ($\lambda_{threshold}$ = 2461.752 nm) shows a same shape as Figure 2a). A similar shape as for λ = 2025 nm (full triangle line), has been previously observed from photo detachment of Iodine ion (Blondel et al., 1990). In the Figure 3b), the dotted line (λ = 2461.752 nm) curve displays three maxima 0° (180°) 90° and two minima at 43° (129°). For 3s total cross-sections (Table 3a), our results agree well at threshold with that of Maquet (1977). Unfortunately, for these angular coefficients, there would not yet exist calculated data obtained from other methods; and that prevents us from testing the reliability of our results for 2p (3.2.1.2) and 3p states. Let us now study the case of circularly polarization.

Circular polarization

Whatever the Tables 1a), 2a) or 3a), for ns states, only one coefficient occurs: d'; the corresponding total cross-sections $\frac{\sigma'_{n,s}}{I^2}$ (Table 1b) agree well with that obtained from other methods (Maquet, 1977; Kristenko and Vetchinkin, 1976; Laplanche et al., 1976; Gao and Starace, 1988). In Figure 1, for λ = 250 nm (dashed line), the distribution is peaked at θ = 90° (angle between the light propagation direction and that of the ejected photoelectron) and it follows a d'sin^{6}θ, behaviour.

In contrast, Tables 2b) and 3b), show for np states two coefficients c'and d'; but in this case, the last one can take either a positive or negative value; this would mean that, the destructive interference terms appearing in Equation (39) always cancels the quadratic term.

Furthermore, except for a few wavelengths, c' is always much stronger than d'; that would be due to the occurrence in Equation (38), of the quadratic terms corresponding to the four opened channels. Then, one would expect to have a pronounced c'sin^{4}θ distribution. We have not shown all the curves, but they exhibit the same shape as Figure 2b) for λ = 860 nm (dashed line); which in turn is similar to Figure 1, for λ = 250 nm (dashed line). A direct consequence from these behaviours is: if for ns states all the photoelectrons are ejected as F-waves, for np states, most of them would be ejected as D-waves.

Our 2p and 3p total cross-sections (cm^6W^{-2}) values (Tables 2b) and 3b)), agree well at threshold, with the values: $\frac{\sigma'_{2p}}{I^2} = 1.48(-41)$ for $\lambda = 1094.112$ nm; and $\frac{\sigma'_{3p}}{I^2} = 6.22(-39)$ for $\lambda = 2461.752$ nm; obtained by Maquet (1977).

Conclusion

Within the framework of perturbation theory and of dipole approximation, we have shown that, the angular distribution for third order processes can be expressed for any initial state of quantum numbers n, l of the hydrogen atom as: $a + b\cos^2\theta + c\cos^4\theta + d\cos^6\theta$; whatever the polarization (linear or circular). From the explicit expressions of ns and np initial states, it is shown for the particular case of linear polarization that the isotropic term rigorously vanishes for ns states, but, subsists only for any initial state with an orbital quantum number greater than zero and contains twenty one contributing terms for np states. In the case of circular polarization the distribution follows a sin^{6}θ behaviour for ns states, while for np initial states it is analytically expressed as a combination of sin^{4}θ and sin^{6}θ.

From the quantitative analysis where a wide range of laser wavelengths including the ionization threshold are considered, it is shown that: for linear polarization the shapes are strongly dependent on both quantum numbers n, l and the wavelength; while for circular polarization the shapes remain the same even if the behaviour is either sin^{6}θ (ns states) or sin^{4}θ (np states). It is also shown that at θ = 0° or 90° the distribution is

strongly affected by the weights of the competing outgoing channels. Furthermore, our total cross-sections are globally in good agreement with that obtained from other methods for ns states; and further data for np states are much needed as a test of the validity of the theory. These results can be applied to more complex atoms. In the near future, we hope to extend these calculations above threshold ionization and to higher order processes.

REFERENCES

Arnous E, Klarsfeld S, Wane ST (1973). AngularDistribution in the two – Quantum Atomic Photo effect Phys. Rev., A7: 1559-1568.

Blondel C, Crance M, Delsart C, Giraud A (1990). "Multiphoton Process" (Proc 5th Int. conf. 24-28 Sept. Paris on Multiphoton Processus) Ed. by Mainfray G. and Agostini P, pp. 59-68.

Chen CT, Robicheaux F (1996). R. matrix Floquet description of multiphoton ionization of Li. Phys Rev., A 54: 3261-3269.

Cooper J, Zare RN (1969). Atomic Collision Processes in lectures in theoretical Physics XI-C. Ed. Geltma S., Mahanthapa K. T. and Brittin W. E. (Gordon and Breach, New York, pp. 317-337.

Dodhy A, Compton RN, Stockdale JAD (1985). Photo electron Angular Distribution for Near-threshold Two-Photon Ionization of Cesium and Rubidium Atoms Phys. Rev. Lett., 54: 422-425.

Dodhy A, Compton RN, Strockdale JAD (1986). Multiphoton ionization of rubidium atoms near the $4d^2$ D quadrupole transition Phys Rev A, 33: 2167-2170.

Fabre F, Agostini P, Petite G, Clement M (1981). Angular distribution in above -Threshold ionization of Xe at 0.53 µm; J. Phys. B: At. Mol. Phys., 14: L677-L681.

Gao B, Starace FA (1988). Variational calculation of Multiphoton Processes for H atom. ; Phys. Rev. Lett., 61: 404-407.

Giugni A, Cavalieri S, Eramo R, Fini L, Matarezzi M (2000). Electron angular distribution in non resonant three – photon ionization of Xenon. J. Phys. B.: At. Mol. Opt. Phys., 33: 285-289.

Gontier Y, Rahman NK, Trahim M (1975). Differential cross section of multiphoton ionization. J. Phys. B: Atom. Mol. Phys., 8: L179-L182.

Gontier Y, Rahman NK, Trahim M (1986). Calculations of total cross section and angular distribution of threshold and above threshold ionization of atomic Hydrogen at the fourth harmonic of a Nd^{3+} glass laser. Phys. Rev., A 34: 1112-1116.

Gontier Y, Trahim M (1971). Multiphoton Processes in a Hydrogen Atom; Phys. Rev A., 4: 1896-1906.

Khristenko SV, Vetchinkin SI (1976). Opt. Spectrosk. 40: 417(Engl. Transl. 1976).

Klarsfeld S, Maquet A (1972). Circular versus Linear Polarization in Multiphoton Ionization Phys. Rev. Lett., 29: 79-81.

Lambropoulos P (1972). Effect of Light Polarization on Multiphoton Ionization of Atoms. Phys. Rev. Lett., 28: 585-587.

Lambropoulos P (1972). Multiphoton Ionization of one Electron Atoms with circulary polarized light. Phys. Rev. Lett., 29: 453-455.

Lambropoulos P, Tang X (1986). Comment on "Photoelectron angular distributions for near Threshold two photon ionization of cesium and Rubidium atoms". Phys. Rev. Lett., 401-401.

Laplanche G, Durrieu A, Frank Y, Jaouen M, Rachman A (1976). The infinite summations of perturbation theory in atomic multiphoton ionization. J. Phys. B., 9: 1263-1277.

Leuch G, Smith SJ (1982). Five photon non resonant photoionization of atomic sodium – the angular distribution photoelectrons. J. Phys. B., At. Mol. Phys., 15: 1051-1059.

Maquet A (1977). Use of the Coulomb Green's function in atomic calculations: Phys. Rev., 15: 1088-1108.

Morellec J, Normand D, Petite G (1982). Non resonant Multiphoton ionization of Atoms. Adv. Atomic Mole. Phys., 18: 97-163.

Potvliege RM, Shakeshaft R (1988). Nonperturbative calculation of partial differential rates for multiphoton ionization of a hydrogen atom in a strong laser field. Phys. Rev. A., 38: 1098-1100.

Radhakrishan R, Thayyullathil RB (2004). Non resonant multiphoton ionization in atomic hydrogen. Phys. Rev. A., 69: 033407-1- 033407-5.

Sobel' Man (1972). Introduction to the Theory of Atomic Spectra: Pergamon Press (Oxford, New York, Toronto, Brauschweig).

Yang CN (1948). On the Angular Distribution in Nuclear Reaction and Coincidence Measurements. Phys. Rev., 74: 764-772.

Zernik W, Klopfenstein RW (1965). Two-photon Ionization of Atomic Hydrogen. J. Math. Phys., 6: 262-269.